Electronic band structure of indium tin oxide and criteria for transparent conducting behavior

O. N. Mryasov* and A. J. Freeman
Materials Research Center and Department of Physics and Astronomy, Northwestern University, Evanston, Illinois 60208-3112
(Received 26 September 2000; revised manuscript received 15 November 2000; published 3 December 2001)

Indium-based transparent conductors, notably indium tin oxide (ITO), have a wide range of applications due to a unique combination of visible light transparency and modest conductivity. A fundamental understanding of such an unusual combination of properties is strongly motivated by the great demand for materials with improved transparent conducting properties. Here we formulate conditions for transparent conducting behavior on the basis of the local density full-potential linear muffin-tin orbital electronic band structure calculations for Sn-doped In_2O_3 and available experimental data. We conclude that the position, dispersion, and character of the lowest conduction band are the key characteristics of the band structure responsible for its electro-optical properties. Further, we find that this lowest band is split with Sn doping due to the strong hybridization with dopant *s*-type states and this splitting contributes to both the decrease of the plasma frequency and the mobility of the carriers.

DOI: 10.1103/PhysRevB.64.233111 PACS number(s): 71.20.−b

Tin-doped In_2O_3 (ITO) exhibits a unique combination of optical and electrical transport properties: (i) high optical transparency in the visible range ($>80\%$) and (ii) low resistivity of the order of $10^{-4}\Omega$ cm. While this type of doped oxide material has been widely used for various optoelectronic applications, the insistant demand for better quality materials over the years has inspired research targeted on understanding the mechanisms driving the peculiar combination of observed optical and electrical transport properties. It is generally accepted, despite the observed high sensitivity of its properties on processing conditions,[1] that the electronic band structure is the one of the most important factors for understanding the unique interplay between optical absorption and conductivity in these materials. Thus, most of the interesting transparent oxide properties are predetermined and can be satisfactorily described on the microscopic level only on the basis of a sufficiently detailed and reliable model of the electronic band structure.

Despite its importance, however, the electronic structure of ITO has not been investigated thoroughly. Several spectroscopic and optical measurements were undertaken to elucidate its electronic structure and electron scattering mechanisms. Fan and Goodenough proposed a schematic energy band model for pure and doped In_2O_3 on the basis of their electron spectroscopy for chemical analysis (ESCA) measurements.[2] Despite its very schematic character, this model is still the only existing basis for qualitative explanations of the observed high optical transparency in this material. Clearly, both a more realistic model of the electronic structure (with reasonable dispersion) and a detailed quantitative analysis of the corresponding optical properties are required for further advances in understanding its unusual properties. Results of the analysis of optical and transport properties for a one-dimensional model of the electronic structure, with effective masses taken from measurements, were reported by Hamberg *et al.*[3] Unfortunately, there is no justification that this very simple model of the electronic band structure is sufficiently reliable. Indeed, due to the ambiguity of the interpretation of the experimental data and sample preparation problems, the electronic band structure suggested on the basis of these experimental studies is not sufficiently detailed and may not be accurate.

Thus, it is highly desirable to make use of modern *ab initio* methodologies for accurate and detailed band structure calculations to compensate for the shortcomings of existing model theoretical and experimental studies. Such calculations are quite challenging, however, due to the complexity of the lattice structure and electronic interactions in these compounds. To our knowledge, the only *ab initio* band structure calculations available for pure In_2O_3 were performed using the linear muffin-tin orbital method with the atomic sphere approximation (LMTO-ASA).[4] Overall, the results obtained are in agreement with available spectroscopic measurements but several open questions remain—related to the reliability of the ASA approximation for such open structures. On the other hand, cluster calculations are unlikely to be able to compensate fully for the lack of *ab initio* band structure calculations for Sn-doped In_2O_3 due to finite cluster size effects and difficulties in interpreting results of cluster methods in terms of the optical and transport properties.[5] Unfortunately, band structure calculations of the Sn-doped In_2O_3 have not yet been reported.

In this paper, we present the first no-shape approximation, electronic band structure calculations for both pure and Sn-doped In_2O_3 using the accurate and relatively numerically efficient, full potential linear muffin-tin orbital (FLMTO) method.[6–8] We focus on details of the electronic band structure (common for all well-known parent materials for TCO's such as In_2O_3, SnO_2, and ZnO) which can be related to the unusual combination of their optical and electrical transport properties. In particular, we find that (i) the position and (ii) the dispersion and character of the highly dispersed band at the bottom of the conduction band are the most important features of the host electronic band structure which provide necessary conditions for transparent conducting behavior with electron doping.

The first-principles (FLMTO) calculations were performed for both In_2O_3 and ITO with the full 40 atoms/cell, including 24 empty spheres to ensure a good packing ratio, and a correspondingly accurate representation of the charge

 ©2001 The American Physical Society

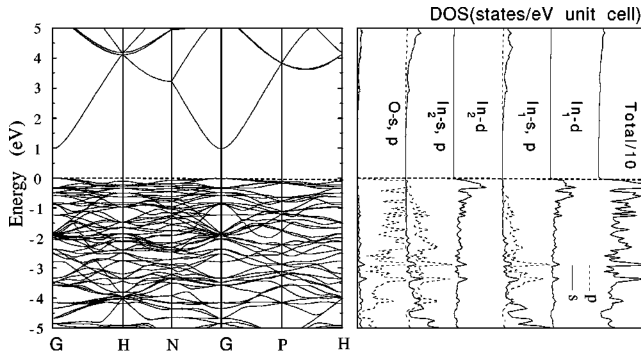

FIG. 1. Electronic band structure (left panel) and projected density of states (right panel) for In_2O_3.

density in the interstitial region with a triple-kappa basis, $\kappa_1^2=-0.01$, $\kappa_2^2=-1.0$, and $\kappa_3^2=-2.3$ Ry. We used the Ceperly-Alder form for the exchange-correlation potential. Integration over $\vec{k}$ space was performed using $4\times4\times4$ divisions of the Brillouin zone. In order to check the accuracy of this computational setup, we first performed calculations of the equilibrium volume of In_2O_3 which turned out to be 0.965 of the experimental unit cell volume. This deviation from experiment is typical of the local density approximation (LDA) and corresponds to an equilibrium lattice constant $a_{th}=18.900$ a.u, to be compared with experiment $a_{exp}=19.125$ a.u.

The band structure (along high symmetry lines in the Brillouin zone) and projected density of states for pure In_2O_3 are presented in Fig. 1. Our results show the existence of the direct band gap of about 1 eV for the experimental lattice constant and about 1.5 eV for the theoretical equilibrium volume — which is typically underestimated by the LDA [to be compared with the experimental optical band gap of 3.6 eV (Ref. 3)]. As can be seen from the calculated projected density of states and character of the bands, the main contribution to the top of the valence band comes from O $2p$ states hybridized with $In_2 5d$ while the bottom of the conduction band is mainly formed from In_1 and $In_2 5s$ electronic states hybridized with O $2s$ states. This feature of the electronic band structure is apparently in disagreement with the model band diagram by Fan and Goodenough[2] suggesting a gap between the In $5s$ and In $5p$ states.

The remarkable feature of the calculated In_2O_3 band structure is the single free-electron-like band of s character (mixed In_2, oxygen, and In_1 states) forming the very bottom of the conduction band, which in turn is separated at the Γ point in the Brillouin zone by a 4 eV gap from a higher energy band having mixed O $2p$ and In $5s$ character. The high dispersion of this band appears to explain the pronounced observed Burstein-Moss (BM) or shift or shift of the optical absorption edge with sufficient doping.[11] The high dispersion and s-type character of this band may also explain the high conductivity due to the high mobility of these states. The s-type character of these states results in a rather uniform distribution of their electronic charge density and so to their relatively low scattering. The high dispersion of this band is predetermined by a strong hopping integral between neighboring In sites. We shall see next from calculations of the band structure for Sn-doped In_2O_3 that the above surmises, based on the results for pure In_2O_3, are in fact correct.

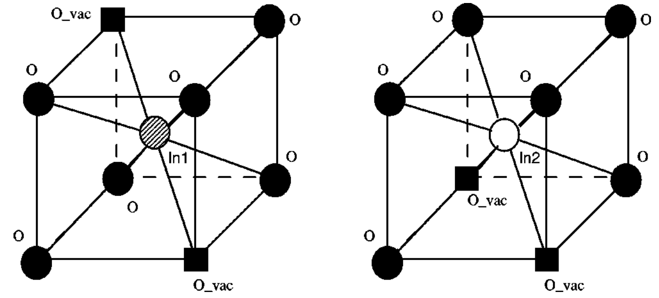

FIG. 2. Schematic illustration of atomic arrangements in In-O octahedra for In_1 and In_2 sublattices. The oxygen atoms are denoted by solid circles, In_1 atoms by shaded circles, In_2 as open circles, and oxygen vacancies by solid squares.

Since In_2O_3 crystallizes in the ordered vacancy structure with 8 formula units, replacement of 1 out of 16 indium atoms by Sn corresponds to a 6.5% level of doping — which is about the limit of solubility reported for this material. As can be seen in Fig. 2, some of the In atoms (4/16) occupy the centers of the trigonally distorted octahedra (Wycoff $8b$ positions or In_1) and others (12/16) occupy the centers of tetragonally distorted octahedra (Wycoff $24d$ positions or In_2). Thus, to elucidate the role of substitutional disorder in In sublattices we performed calculations of the electronic band structure for two cases when Sn substitutes in the In_1 and In_2 sublattices. Once again, to check the accuracy of our computational setup, we performed preferred site total energy calculations and found that Sn substitution into In_1 sublattice is lower in energy by about 3.7 mRy per unit cell. This result is consistent with recent Reitvelt[9] and earlier Mössbauer[10] measurements.

The band structure (along high-symmetry lines in the Brillouin zone) and projected density of states for Sn-doped In_2O_3 are presented in Fig. 3. In addition to (i) the pronounced BM shift which by far compensates (ii) the slight lowering of the fundamental band gap due to the many-body effect[3] expected from the band structure of pure In_2O_3, we find that doping also opens an additional band gap which splits the free-electron-like band due to the strong hybridization between Sn and In s states. This hybridization gap con-

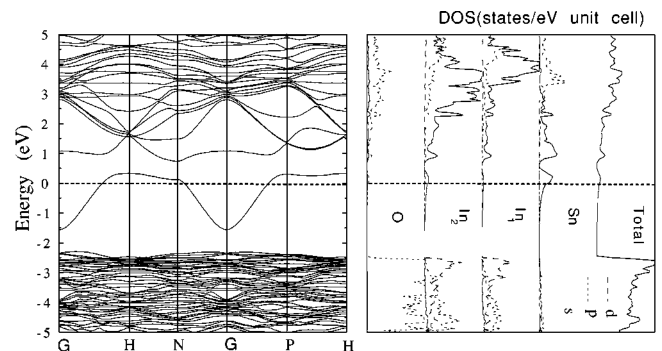

FIG. 3. Electronic band structure (left panel) and projected density of states (right panel) for Sn-doped In_2O_3.

tributes to the lowering of the optical absorption due to interband transitions. Experimental data[12] and the fact of low optical absorption itself suggest that the plasma frequency ω_p, given by the expression

$$\omega_p^2 = \frac{8\pi e^2}{3\Omega} \sum_{\vec{k}\lambda} |\vec{V}_{\vec{k}\lambda}|^2 \delta(E_{\vec{k}\lambda} - E_F) \quad (1)$$

(where $\vec{V}_{\vec{k}\lambda} = \langle \vec{k}\lambda | \nabla | \vec{k}\lambda \rangle$ is the velocity of an electron in state $|\vec{k}\lambda\rangle$ and Ω is the volume of the Brillouin zone), is below the optical range. The opening of the second gap effectively lowers ω_p since it is roughly proportional to the largest intraband transition energy. On the other hand, the appearance of the hybridization gap effectively decreases the dispersion of the *s*-type band that in fact corresponds to the observed decrease of the carrier mobility (in addition to ionized impurity scattering effects[11]) with concentration.

The band structure presented in Fig. 3 corresponds to a doping level of 6.5% with Sn atoms in the In_1 sublattice. Note, however, that the band structure in the case of Sn doping in the In_2 sublattice is very similar, even quantitatively in terms of the dispersion and position of the band and second gap, to the one with Sn substituting In in the In_1 sublattice (Fig. 3). Thus, the main features of the band structure we discuss here—namely, the character, dispersion, and position of the highly dispersed band and second gap—are not expected to be modified qualitatively due to substitutional disorder (i.e., a random distribution of the Sn atoms between the In_1 and In_2 sublattices).

To summarize, on the basis of the calculated band structure of pure and Sn-doped In_2O_3 (and of ZnO and SnO_2, not reported here), we formulate the following conditions of that favor transparent conducting behavior: (i) a highly dispersed and single character *s*-type band at the bottom of the conduction band, (ii) this band is separated from the valence band by a large enough fundamental band gap to exclude interband transitions in the visible range, and (iii) the properties of this band are such that the plasma frequency is below the visible range. The first condition provides, in fact, the high mobility of the extra carriers introduced by the dopant, a pronounced BM shift which helps to keep intense interband transitions from the valence band out of the optical range (provided the fundamental band gap is large enough) and a relatively low intensity of the interband transitions from the partially occupied band at the top of conduction band (partially due to the second gap and *s*-type character; see Fig. 3). We note that the splitting of the highly dispersed band with doping helps to satisfy requirement (iii) and also reduces the contribution of the interband transitions. We note also that the *s* character of the highly dispersed band also favors lower absorption due to the smaller matrix elements of the momentum operator (radial derivatives for lower *l* quantum numbers are smaller). The splitting of the conduction band into a second gap also plays a role in favor of lower absorption due to transitions from the occupied part of the highly dispersed band to the unoccupied part.

Work at Northwestern University was supported by the NSF (through the N.U. Materials Research Center) and at Sandia National Laboratories by the Office of Basic Energy Science, Division of Materials Science, of the U.S. Department of Energy under Contract No. DE-AC04-94AL85000.

*Present address: Sandia National Laboratories, Mail Stop 9161, P.O. Box 0969, Livermore, CA 94551-0969. Electronic address: onm@pluto.phys.nwu.edu.

[1] Z.M. Jarzebski, Phys. Status Solidi A **71**, 13 (1982).
[2] J.C. Fan and J.B. Goodenough, J. Appl. Phys. **48**, 3524 (1977).
[3] I. Hamberg, C.G. Granquist, K.F. Berggren, B.E. Senelius, and L. Engstrom, Phys. Rev. B **30**, 3240 (1984).
[4] H. Odaka, S. Iwata, N. Taga, S. Ohnishi, Y. Kaneta, and Y. Shigesato, Jpn. J. Appl. Phys., Part 1 **36**, 5551 (1997).
[5] I. Tanaka, M. Mizuno, and H. Adachi, Phys. Rev. B **56**, 3536 (1997).
[6] M. Methfessel, Phys. Rev. B **38**, 1537 (1988).
[7] M. Methfessel, C.O. Rodriguez, and O.K. Andersen, Phys. Rev. B **40**, 2009 (1989).
[8] A.T. Paxton, M. Methfessel, and H. Polatoglu, Phys. Rev. B **41**, 8127 (1990).
[9] N. Nadaud, N. Lequeux, M. Nanot, J. Love, and T. Roisnel, J. Solid State Chem. **135**, 140 (1998).
[10] K. Nomura, Y. Ujihira, and S. Tanaka, Hyperfine Interact. **42**, 1207 (1988).
[11] I. Hamberg and C.G. Granquist, J. Appl. Phys. **60**, R123 (1986).
[12] T. Gerfin and M. Gratzel, J. Appl. Phys. **79**, 1722 (1996).